Published OnlineFirst July 1, 2016; DOI: 10.1158/1535-7163.MCT-16-0136

Small Molecule Therapeutics

Molecular Cancer Therapeutics

Covalent Targeting of Fibroblast Growth Factor Receptor Inhibits Metastatic Breast Cancer

Wells S. Brown[1], Li Tan[2], Andrew Smith[1], Nathanael S. Gray[2], and Michael K. Wendt[1]

Abstract

Therapeutic targeting of late-stage breast cancer is limited by an inadequate understanding of how tumor cell signaling evolves during metastatic progression and by the currently available small molecule inhibitors capable of targeting these processes. Herein, we demonstrate that both β3 integrin and fibroblast growth factor receptor-1 (FGFR1) are part of an epithelial–mesenchymal transition (EMT) program that is required to facilitate metastatic outgrowth in response to fibroblast growth factor-2 (FGF2). Mechanistically, β3 integrin physically disrupts an interaction between FGFR1 and E-cadherin, leading to a dramatic redistribution of FGFR1 subcellular localization, enhanced FGF2 signaling and increased three-dimensional (3D) outgrowth of metastatic breast cancer cells. This ability of β3 integrin to drive FGFR signaling requires the enzymatic activity of focal adhesion kinase (FAK). Consistent with these mechanistic data, we demonstrate that FGFR, β3 integrin, and FAK constitute a molecular signature capable of predicting decreased survival of patients with the basal-like subtype of breast cancer. Importantly, covalent targeting of a conserved cysteine in the P-loop of FGFR1–4 with our newly developed small molecule, FIIN-4, more effectively blocks 3D metastatic outgrowth as compared with currently available FGFR inhibitors. *In vivo* application of FIIN-4 potently inhibited the growth of metastatic, patient-derived breast cancer xenografts and murine-derived metastases growing within the pulmonary microenvironment. Overall, the current studies demonstrate that FGFR1 works in concert with other EMT effector molecules to drive aberrant downstream signaling, and that these events can be effectively targeted using our novel therapeutics for the treatment of the most aggressive forms of breast cancer. *Mol Cancer Ther; 15(9); 2096–106. ©2016 AACR.*

Introduction

Fibroblast growth factor receptor (FGFR) is an emerging target for the treatment of triple-negative breast cancer (TNBC), Herceptin-resistant $Her2^+$ breast cancer, and tamoxifen-resistant ER^+ breast cancers (1–4). The FGFR family is composed of 4 tyrosine kinase receptors, FGFR1–4. FGFR1–3 undergo significant alternative splicing resulting in two primary isoforms with different ligand binding sites (-iiib or -iiic) and either full-length (α) or truncated (β) forms of the receptor (5). FGFR1 also undergoes gene amplification and translocation, particularly in the luminal B subtype of breast cancer (6). In addition to gene amplification, transcriptional expression of FGFR1-iiic is dramatically increased by epithelial–mesenchymal transition (EMT; refs. 1, 7, 8). We recently demonstrated that FGFR1 is a unique marker of EMT as its expression remains elevated through the oncogenic reversion of this process, or mesenchymal–epithelial transition (MET; ref. 1). This is a key finding as highly aggressive breast cancer cells can readily transition between epithelial and mesenchymal states (9, 10). Therefore, the maintained upregulation of FGFR1 during epithelial–mesenchymal plasticity contributes to the potential of this growth factor signaling pathway as a therapeutic target for the treatment of metastatic breast cancer. However, it remained to be determined whether enhanced FGFR expression alone is sufficient to drive FGF-mediated metastatic tumor growth or if other aspects of EMT are also required for this process.

In addition to modulated expression of growth factor receptors, another critical aspect of EMT is the production of extracellular matrix proteins and their cognate sensing molecules (11). Along these lines, EMT-mediated upregulation of αvβ3 integrin is well established, as is its ability to interact with TGFβ receptors and EGFR (12, 13). Furthermore, biochemical studies and results from endothelial cells suggest that β3 integrin also can bind to FGFs and may form a ternary complex with FGF and FGFR1 (14–16). Given these previous findings, we hypothesized that β3 integrin and FGFR1 work in concert during EMT to promote the metastatic progression of breast cancer.

To date, nearly all clinically used kinase inhibitors are ATP-competitive, noncovalent compounds whose pharmacodynamics are limited by competition with the large intracellular pool of ATP (17). The recent FDA approval and clinical success of the covalent EGFR inhibitor osimertinib for the treatment of lung cancer and the BTK inhibitor Ibrutinib for the treatment of B-cell–derived tumors serves as a proof-of-principle for the continued development of covalent kinase inhibitors as anticancer therapeutics (18). We recently developed FIIN-2, a potent and selective covalent pan-FGFR–targeting agent that inhibits FGFR1 in biochemical and cellular assays at nanomolar concentrations (19). Despite being very potent in cellular assays, FIIN-2 proved not to be a suitable *in vivo* drug candidate. Therefore, a major objective of the current study was to develop and conduct preclinical, *in vivo* validation of FIIN-4, our newly formulated covalent inhibitor of

[1]Purdue University Center for Cancer Research, Department of Medicinal Chemistry and Molecular Pharmacology, Purdue University, West Lafayette, Indiana. [2]Department of Cancer Biology, Dana-Farber Cancer Institute, Harvard Medical School, Boston, Massachusetts.

Note: Supplementary data for this article are available at Molecular Cancer Therapeutics Online (http://mct.aacrjournals.org/).

Corresponding Author: Michael K. Wendt, Purdue University, 201 South University Street, Hansen Life Sciences Building, West Lafayette, IN 47907. Phone: 765-494-0860; Fax: 765-494-1414; E-mail: mwendt@purdue.edu

doi: 10.1158/1535-7163.MCT-16-0136

Published OnlineFirst July 1, 2016; DOI: 10.1158/1535-7163.MCT-16-0136

FGFR. Taken together, our studies present mechanistic insight into how EMT as a process contributes to FGFR signaling in metastatic breast cancer. Moreover, our findings suggest that β3 integrin, FAK, and FGFR can serve as useful biomarkers for the application of our next-generation, covalent inhibitor of FGFR for the treatment of metastatic breast cancer.

Materials and Methods

Cell lines and reagents

Murine D2.A1 were obtained from Dr. Fred Miller in 2010 (Wayne State University, Detroit, MI), whereas murine 4T1 and NMuMG were purchased from the ATCC in 2008. Bioluminescent 4T1 and D2.A1, cells were engineered to stably express firefly luciferase under the selection of Zeocin as previously described (20). All cell lines were tested and verified via the IMPACT III analysis at IDEXX Bioresearch on April 2, 2014. NMuMG cells expressing Twist and β3 integrin were constructed via stable transduction using pBabe and pMSCV viral particles, respectively. Plasmids encoding the FGFR1–eGFP fusion protein were a kind gift from Michael Stachowiak (Department of Chemistry, State University, Buffalo, NY). Cellular depletion of β1 and β3 integrin expression was achieved by lentiviral transduction of previously verified pLKO.1 shRNA vectors (Thermo Scientific; Supplementary Table S1) as described previously (21). Ectopic expression of FGFR1-α-IIIc was accomplished as previously described and selected for using neomycin (1). The covalent FGFR inhibitor FIIN-2 was synthesized as described previously (19). FIIN4 was synthesized with the same synthetic route as FIIN-2, with 3-nitrobenzylamine instead of 4-nitrobenzylamine as the starting material. PF-562,271 was provided by Pfizer and defactinib was purchased from Selleckchem.

Patient-derived xenografts and *in vivo* drug treatments

Patient tumor tissues (HCI-015) were obtained from the Hunstman Cancer Institute (HCI, Salt Lake City, UT) Preclinical Research Resource (PRR). Transfer of tumor tissues was conducted under Institutional review board approval from both HCI and Purdue University (West Lafayette, IN). Approximately 1 mm^3 pieces of tumor tissue were engrafted onto the mammary fat pads of 4-week-old NSG mice according to published procedures (22). Cohorts of these tumor-bearing mice were treated with FIIN-4 (25 mg/kg) every 48 hours. Mammary tumor sizes were measured using digital calipers and the following equation was used to approximate tumor volume [$V = (\text{length}^2) \times (\text{width}) \times (0.5)$]. In separate experiments, 4-week-old female Balb/c mice were inoculated via the tail vein with *ex vivo* 4T1-L4 pulmonary metastases. These pulmonary tumor-bearing mice were similarly treated with FIIN-4. In both cases, FIIN-4 was originally suspended in DMSO and then further diluted in a solution 0.5% carboxymethyl cellulose and 0.25% Tween-80 to a final concentration of 10% DMSO for administration to animals via oral gavage. All animal experiments were conducted under Institutional Animal Care and Use Committee approval from Purdue University.

Immunoassays

For signaling assays, cells were serum deprived for 6 hours (NMuMG) or overnight (D2.A1) in the presence or absence of the indicated inhibitors and cells were subsequently stimulated with the indicated growth factors. For immunoblot assays, lysates generated from two-dimensional (2D) and three-dimensional (3D) cultures were prepared as described previously (23). Antibodies used herein are described in the Supplementary Table S2. For immunocytochemistry, cells were fixed in 4% formalin, blocked, and stained with the indicated antibodies (Supplementary Table S2). For GFP-Trap experiments (GFP-Trap_A, Chromo-Tek), cells were rinsed in 1% formaldehyde, lysed in 1 mL membrane co-IP buffer [50 mmol/L TRIS, 15 mmol/L EGTA, 100 mmol/LNaCl, 0.1% Triton X-100, pH 7.5, and protease inhibitor cocktail (Sigma) added just before use], and 20 μL of supernatant was saved for input control. IHC images of FGFR1 in patient tumors were gathered from the human protein atlas (24, 25).

mRNA transcript analyses

For real-time PCR analysis, NMuMG cells were stimulated with TGF-β1 (5 ng/mL) for 48 hours, at which point total RNA was isolated using the RNeasyPlus Kit (Qiagen). Alternatively, RNA was similarly isolated from 4T1 *in vitro* cultured cells or *ex vivo* lung metastases. Afterward, total RNA was reverse transcribed using the iScriptcDNA Synthesis System (Bio-Rad), and semiquantitative real-time PCR was conducted using iQ SYBR Green (Bio-Rad) as described previously (23). For identification of the FGFR splice variants, PCR products were visualized by gel electrophoresis. The oligonucleotide primer pairs used have been described previously (1).

Enzymatic assays

The enzymatic activities against FGFR1–4 were tested in Z'-Lyte assays with ATP concentrations of K_m for each kinases; all the protocols are available from Life Technologies (www.invitrogen.com/drugdiscovery/).The MLM stability assays were previously reported and are commercially available from Scripps Florida (26).

In vivo pharmacokinetic studies

Male Swiss albino mice were dosed via oral gavage (0.1% v/v Tween 80, 0.5% w/v NaCMC in water at a dose of 10 mg/kg) or via intravenous tail vein injection (suspensions in 5% NMP, 5% solutol HS in normal saline at a dose of 2 mg/kg). Blood samples were collected at 0.08, 0.25, 0.5, 1, 2, 4, 8, and 24 hours (intravenously) and at predose, 0.25, 0.5, 1, 2, 4, 6, 8, and 24 hours (orally). Plasma samples were separated by centrifugation of whole blood and stored below −70°C until bioanalysis. All samples were processed for analysis by protein precipitation using acetonitrile and analyzed with fit-for-purpose LC/MS-MS method (LLOQ, 1.06 ng/mL). Pharmacokinetic parameters were calculated using the noncompartmental analysis tool of WinNonlin Enterprise software (version 6.3).

Cell biological assays

Cell viability assays were performed using the CellTiter Glo assay according to the manufacturer's instructions (Promega). Visualization of the actin cytoskeleton was performed by staining fixed cells with FITC-conjugated Phalloidin according to the manufacturer's instructions (Thermo Scientific). FGFR1–4 transformed Ba/F3 cell viability assays were conducted via services from Carna Biosciences (http://www.carnabio.com).

3D-organotypic growth assays

Cells were diluted in complete media supplemented with 5% Cultrex (Trevigen) and seeded onto solidified Cultrex cushions (50 μL/well) contained in 96-well plates (1×10^4 cells/cm^2).

Published OnlineFirst July 1, 2016; DOI: 10.1158/1535-7163.MCT-16-0136

Cultrex cushions were supplemented with fibronectin or Collagen I where indicated. Longitudinal bioluminescent growth assays were performed as described previously (1, 23, 27).

Kaplan–Meier plots

The MTCI BreastMark, an online biomarker validation tool (http://glados.ucd.ie/BreastMark/) was used to estimate survival probabilities for breast cancer patients split into two groups based on *ITGB3*, *PTK2*, and *FGFR1* gene expression. This analysis performed by extracting gene expression values and overall patient survival data from 714 basal-like breast cancers.

Statistical analyses

Statistical values were defined using an unpaired Student *t* test, where a *P* value of <0.05 was considered significant. Statistically significant differences in the overall survival of 4T1-pulmonary tumor–bearing mice were analyzed using a log-rank test and a two-way ANOVA test. *P* values for all experiments are indicated.

Results

Twist-mediated induction of EMT enhances FGFR signaling in mammary epithelial cells

We and others have previously demonstrated that FGFR1 is upregulated during the process of TGFβ1-induced EMT (Fig. 1A; refs. 1, 8). Consistent with these findings, pretreatment with TGFβ1 facilitates FGF2-mediated phosphorylation of Erk1/2 (Fig. 1B). We next sought to define the downstream mechanisms responsible for increased expression of FGFR1 during induction of EMT. Similar to TGFβ1 treatment, expression of the basic helix-loop-helix transcription factor Twist also led to a robust induction of EMT in the NMuMG cell model, which included the upregulation of the –iiic splice variant of FGFR1 (Fig. 1A and C and Supplementary Fig. S1). Importantly, expression of Twist did not cause a corresponding decrease in FGFR2, an event that is characteristic of TGFβ-induced EMT, and expressions of FGFR3 and 4 were not affected by Twist or TGFβ (Supplementary Fig. S1; ref. 28). However, similar to TGFβ1-induced EMT, a Twist-mediated EMT event was also sufficient to enhance FGF2-induced phosphorylation of Erk1/2 (Fig. 1D). These findings demonstrate that EMT events that include enhanced FGFR1 expression can facilitate a differential response to subsequent FGF2 ligand stimulation.

β3 integrin redistributes FGFR1 and promotes FGF2 signaling

We next sought to elucidate the impact of EMT on FGFR1 subcellular localization and signaling capacity. Immunofluorescent staining in combination with confocal microscopy revealed that FGFR1 was localized throughout Twist-expressing NMuMG cells (Fig. 1E). To delineate the influence of the overall EMT event on this localization profile of FGFR1, NMuMG cells were stably transfected with an FGFR1–eGFP fusion construct and appropriate FGFR1 expression levels were isolated by FACS (Fig. 2A and Supplementary Fig. S2). In contrast with the localization of endogenous FGFR1 that is induced upon Twist-mediated EMT, ectopic expression of FGFR1 predominantly localized at the cell–cell junctions in NMuMG cells (Figs. 1E and 2A). However, upon recombinant expression of β3 integrin FGFR1–eGFP displayed more diffuse localization throughout the cell that was very similar to what was observed for endogenous FGFR1 upon expression of Twist (Figs. 1E and 2A). To further characterize this pronounced

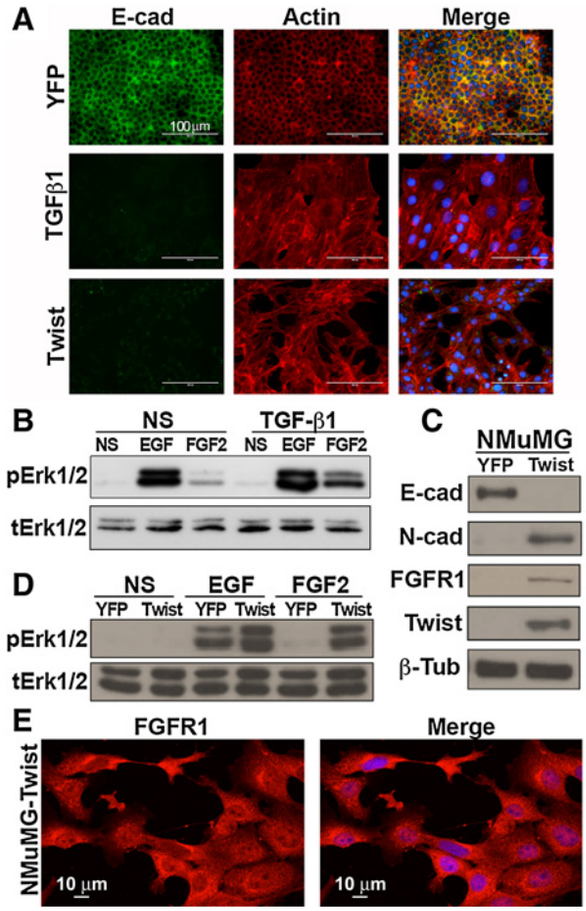

Figure 1.

Twist-mediated induction of EMT enhances FGF2 signaling in mammary epithelial cells. **A,** NMuMG cells expressing YFP were either not stimulated or stimulated for 48 hours with TGFβ1 (5 ng/mL). These cells were stained for expression and localization of E-cadherin (E-cad) or the actin cytoskeleton. Similarly, NMuMG cells were stably transduced with Twist to drive a morphologically similar EMT event. **B,** NMuMG cells were pretreated with TGFβ1 as in **A** and subsequently stimulated with either EGF (50 ng/mL) or FGF2 (20 ng/mL) for 30 minutes. These cells were then analyzed by immunoblot for downstream phosphorylation of Erk1/2. Expression of total Erk1/2 was analyzed as a loading control. **C,** expression of the EMT markers N-cadherin (N-cad) and E-cadherin (E-cad) as well as FGFR1 were analyzed by immunoblot in control (YFP) and Twist-expressing NMuMG cells. Twist and β-tubulin (β-tub) served as loading controls. **D,** NMuMG cells expressing YFP or Twist as shown in **C** were stimulated with either EGF or FGF2 and downstream phosphorylation of Erk1/2 was assessed by immunoblot. Expression of total Erk1/2 was analyzed as a loading control. **E,** Twist-expressing NMuMG cells were stained for expression and localization of FGFR1 and DAPI to visualize the nuclei. All data in **A–E** are representative of at least three independent experiments yielding similar results. Images in **A** were collected on an EVOS FL fluorescence microscope, whereas images in **E** were collected on a Nikon A1R confocal microscope.

change in subcellular localization, we conducted GFP precipitation experiments using cells expressing the FGFR–eGFP fusion construct (Fig. 2B). Consistent with our fluorescence images, we observed FGFR1 to be in complex with E-cadherin (E-cad) under control conditions, but upon coexpression with β3 integrin, FGFR moved out of this complex and was observed to interact with β3 integrin itself (Fig. 2B). These cell culture data are supported by

Published OnlineFirst July 1, 2016; DOI: 10.1158/1535-7163.MCT-16-0136

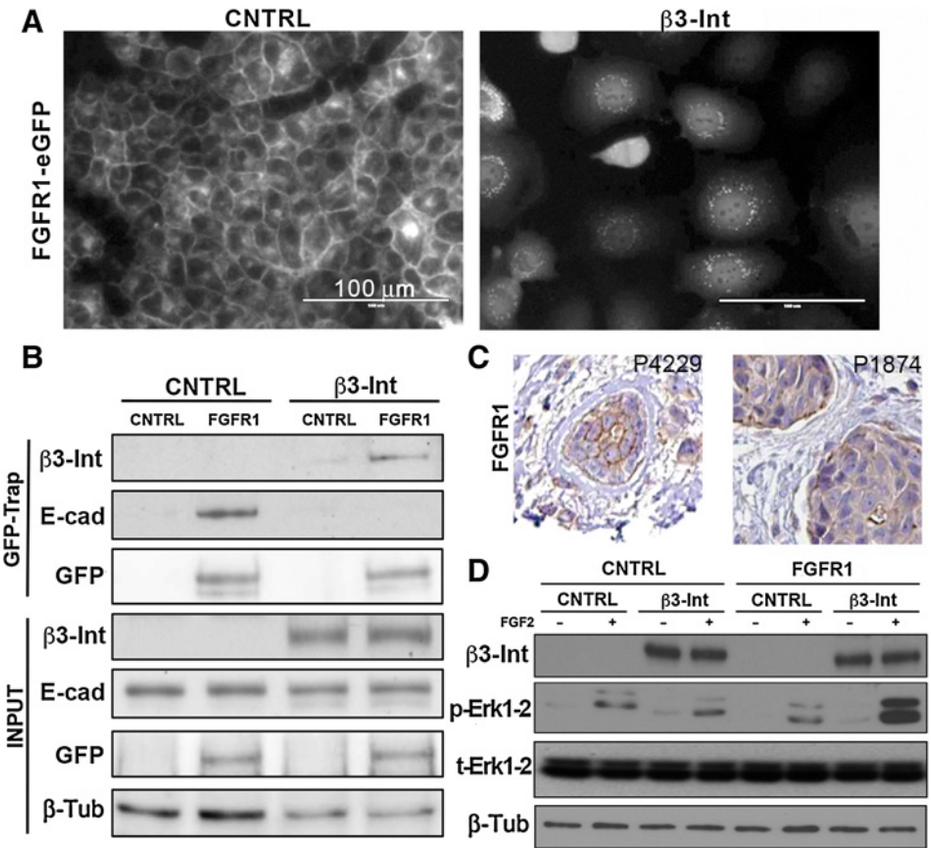

Figure 2.

β3 integrin redistributes FGFR1 and promotes FGF2 signaling. **A,** NMuMG cells were stably transfected with an FGFR1–eGFP fusion protein. These cells were subsequently transduced with control or β3 integrin (β3-Int) encoding viral particles. Differential localization of FGFR1–eGFP was observed upon recombinant expression of β3 integrin. **B,** NMuMG cells constructed to express FGFR1–eGFP and/or β3 integrin were lysed and FGFR1–eGFP was precipitated using GFP-TRAP as detailed in the Materials and Methods. FGFR1–eGFP protein complexes were analyzed by immunoblot for the presence of FGFR1–eGFP(GFP), E-cadherin (E-cad), and β3 integrin (β3-Int). Presence of these proteins and β-tubulin (β-tub) in the input lysate served as loading controls. **C,** patient tumor samples isolated from a primary tumor (P4229) and a lymph node metastasis (P1874) demonstrate plasma membrane versus diffuse cellular localization of FGFR1, respectively. **D,** NMuMG cells were constructed to express FGFR1 and/or β3 integrin (β3-Int) and these cells were stimulated with FGF2 (2ng/mL) for 5 minutes. Subsequent to stimulation, cell lysates were analyzed by immunoblot for the phosphorylation of Erk1/2. Presence of β3 integrin, total Erk1/2, and β-tubulin (β-tub) served as loading controls. Data in **A, B,** and **D** are representative of at least three independent experiments yielding similar results. Images in **A** were collected on an EVOS FL fluorescence microscope.

our analysis of the Human Protein Atlas database, which revealed similarly distinct subcellular localizations of endogenous FGFR1 in a primary breast tumor (Patient 4229) as compared with metastatic patient tumor (Patient 1874) isolated from the lymph node (Fig. 2C). The functional consequence of this change in complex localization is evidenced by the requirement of both β3 integrin and FGFR1 to facilitate enhanced pErk1/2 phosphorylation in response to FGF2 (Fig. 2D and Supplementary Fig. S3A). These data suggest that through the process of EMT, upregulation of both FGFR1 and β3 integrin are required for breast cancer cells to aberrantly sense FGF2 as a proliferative factor.

Three-dimensional cell culture increases expression of β3 integrin and enhances FGF2 signaling

To better recapitulate the *in vivo* condition, we next sought to examine FGF2 signaling under 3D culture conditions. When the NMuMG cells were cultured under 3D growth conditions containing basement membrane extract (BME) FGFR1 overexpression alone, irrespective of β3 integrin expression, was sufficient to facilitate acinar filling in response to exogenous FGF2 (Fig. 3A). We were able to quantify this FGF2-mediated growth response using bioluminescence (Fig. 3B). To extend these studies beyond our overexpression systems, we used the metastatic D2.A1 cells, a system we have recently shown responds poorly to FGF2 when cultured on 2D plastic, but is sensitive to FGFR inhibition in 3D culture and *in vivo* (23). Growth of these cells on 2D plastic yields drastically different growth morphologies as compared to 3D culture of the same cells on BME, Fibronectin, or Collagen I (Fig. 3C). Immunoblot analysis of these differential cultures demonstrated a robust upregulation of β3 integrin in 3D culture conditions as compared to 2D (Fig. 3D). Consistent with the notion that FGFR1 and β3 integrin are required for aberrant FGF2 signaling, we observed a dramatic increase in FGF2-induced phosphorylation of Erk1/2 when these cells were cultured under 3D conditions as compared to traditional 2D culture conditions (Fig. 3E).

Published OnlineFirst July 1, 2016; DOI: 10.1158/1535-7163.MCT-16-0136

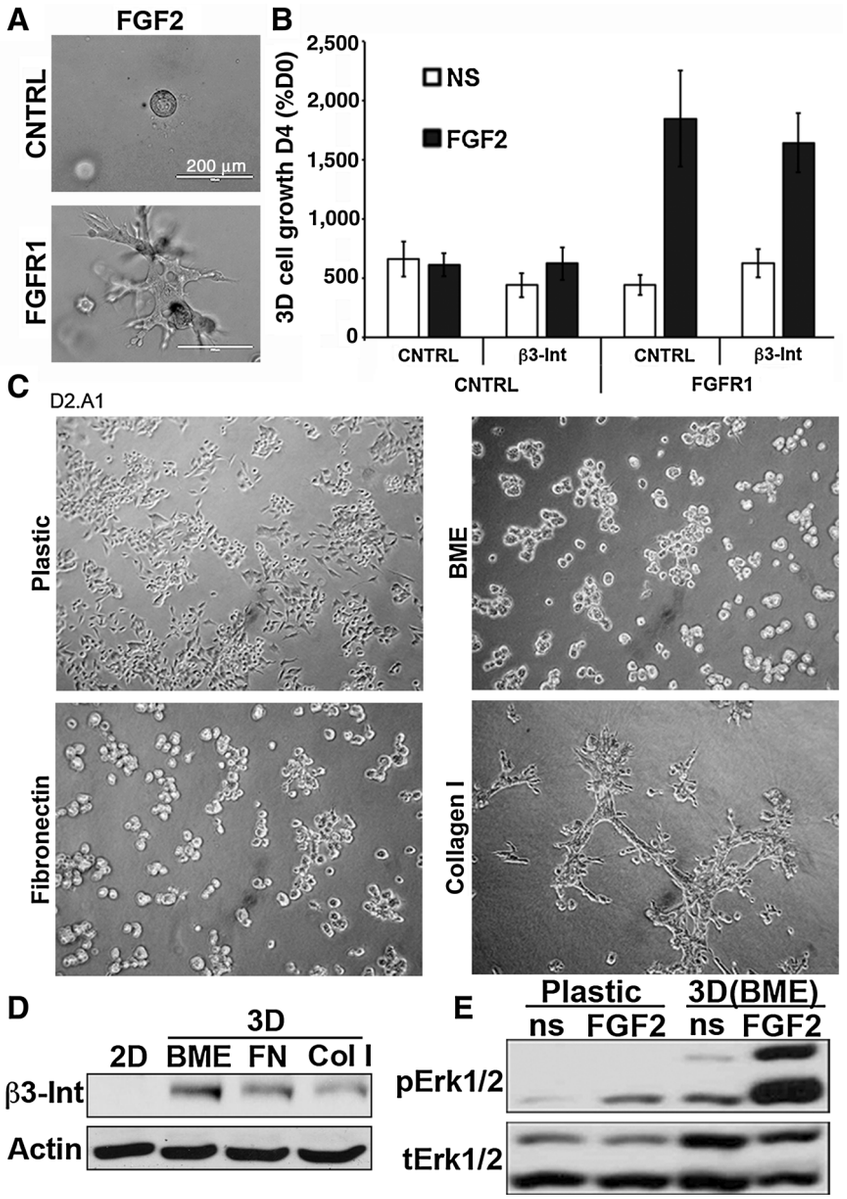

Figure 3.

3D cell culture increases expression of β3 integrin and enhances FGF2 signaling. **A,** control (CNTRL)- and FGFR1-expressing NMuMG cells were grown under 3D culture conditions in the presence of exogenous FGF2 (20 ng/mL) for 10 days. Brightfield images showing the resulting hollow acinar structures (top) and filled structures (bottom) were collected using an EVOS FL microscope. **B,** control NMuMG cells or cells expressing FGFR1 and/or β3 integrin (β3-Int) were cultured in the presence or absence of exogenous FGF2 as in **A** and overall cell growth was quantified by bioluminescence. Data in **B** are the mean ± SD of triplicate wells. Data in **A** and **B** are representative of at least three independent experiments yielding similar results. **C,** metastatic D2.A1 cells were grown on tissue culture plastic or in 3D culture conditions containing BME alone or supplemented with additional Fibronectin or Collagen I as described in the Materials and Methods. Photomicrographs represent typical growth morphologies of these cells when grown in these various conditions. These brightfield images were collected using a TS100 Nikon microscope at ×100 magnification. **D,** following 10 days of culture in the conditions shown in panel **C** (FN, Fibronectin; Col I, Collagen I) cells were lysed and analyzed by immunoblot for expression of β3 integrin (β3-Int). Actin served as a loading control. **E,** D2.A1 cells were cultured on tissue culture plastic or in 3D culture conditions as shown in **C**. These cells were stimulated with FGF2 (20 ng/mL) for 30 minutes and analyzed for downstream phosphorylation of Erk1/2. All data in **C–E** are representative of at least three independent experiments yielding similar results.

Together with our data from the previous figures these findings suggest that EMT in combination with structural changes in the *in vivo* growth environment contribute to upregulation of β3 integrin and the creation of aberrant FGF2 signaling complexes in metastatic breast cancer cells.

β3 integrin is required for FGF2-mediated signaling and 3D cellular outgrowth

Our findings in the NMuMG cell model demonstrated that FGFR1 and β3 integrin were both required for robust FGF2-mediated activation of Erk1/2. To further explore the role of integrins in facilitating FGF2 signaling in metastatic cells, we depleted the expression of either β1 or β3 integrin in the D2.A1 cells using previously established and verified shRNAs (Fig. 4A; ref. 21). As previously observed in other models, depletion of β1 integrin led to a robust compensatory increase in the expression of β3 integrin in D2.A1 cells, but this event did not affect the ability of FGF2 to activate Erk1/2 phosphorylation (Fig. 4A; ref. 21). More importantly, directed depletion of β3 integrin in the D2.A1 cells inhibited the ability of FGF2 to stimulate phosphorylation of Erk1/2 (Fig. 4A and Supplementary Fig. S3B). To better establish the biological significance of these events, we cultured these cells under 3D growth conditions and quantified cellular outgrowth using bioluminescence (Fig. 4B). Addition of exogenous FGF2 enhanced the outgrowth of control D2.A1 cells (Fig. 4B and C). As reported previously, depletion of β1 integrin did lead to a robust inhibition of D2.A1 outgrowth (29). However, this inhibition of basal outgrowth could be completely rescued by the addition of exogenous FGF2, findings that are consistent with the enhanced levels of β3 integrin in these cells (Fig. 4B and C). Finally, directed

Published OnlineFirst July 1, 2016; DOI: 10.1158/1535-7163.MCT-16-0136

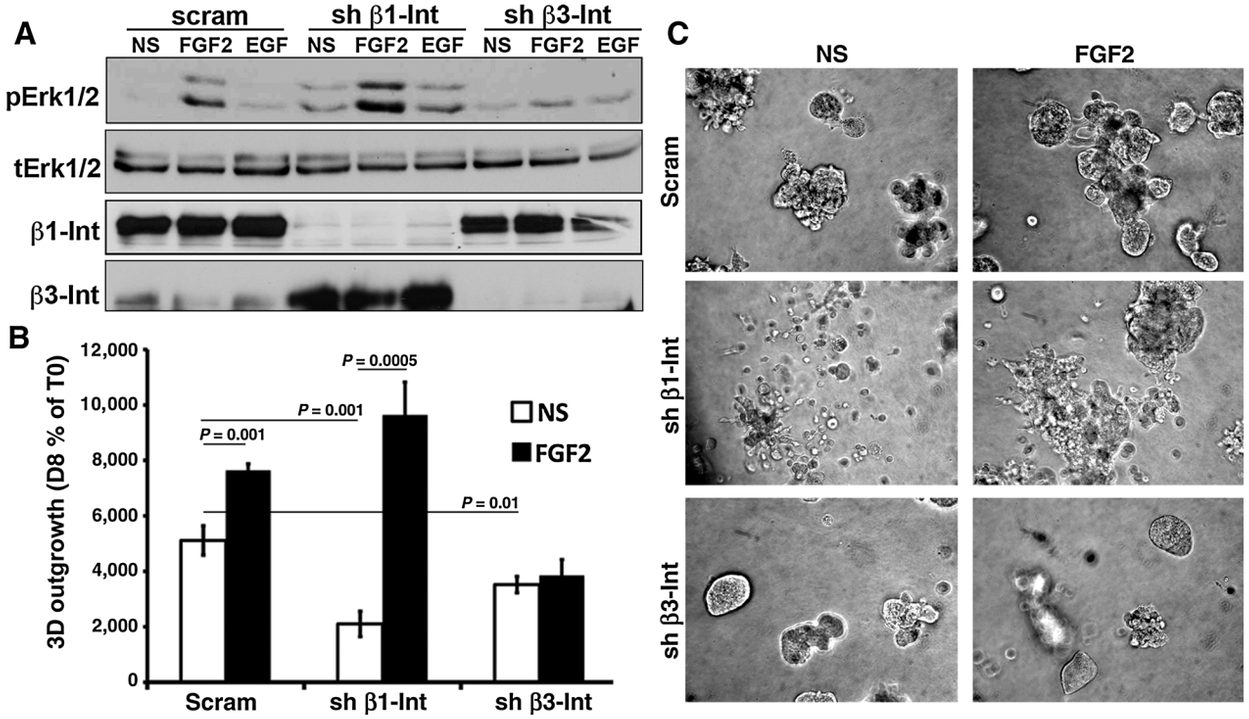

Figure 4.

β3 integrin is required for FGF2-mediated signaling and 3D cellular outgrowth. **A,** D2.A1 cells were depleted for expression of either β1 integrin or β3 integrin using gene-specific shRNAs and these cells were not stimulated (NS) or were stimulated with either EGF (50 ng/mL) or FGF2 (20ng/mL) for 30 minutes and subsequently analyzed by immunoblot for phosphorylation of Erk1/2. Expression of total Erk1/2, β3 and β1 integrin served as a loading control. Data are representative of at least three independent experiments. **B,** D2.A1 cells depleted for β1 or β3 integrin as shown in **A** were cultured under 3D conditions in the presence or absence of exogenous FGF2 (20 ng/mL) for 8 days. Cellular outgrowth under these conditions was quantified by bioluminescence. Changes in cellular outgrowth are shown as the percentage of increase relative to the plated bioluminescent value (T0). Data are the mean values of three independent experiments completed in triplicate resulting in the indicated *P* values. **C,** representative brightfield photomicrographs of the 3D culture conditions described and quantified in **B**. These images were collected using a TS100 Nikon microscope at ×100 magnification.

depletion of β3 integrin similarly lead to a significant inhibition of basal 3D outgrowth by the D2.A1 cells, but unlike depletion of β1 integrin this event completely prevented the ability of exogenous FGF2 to stimulate the outgrowth of the D2.A1 cells (Fig. 4B and C). These data clearly indicate that β3 integrin is necessary for FGF2-mediated 3D outgrowth of metastatic breast cancer cells.

Pharmacologic inhibition of integrin: FGFR signaling blocks three-dimensional metastatic cell growth

Given the critical nature of EMT in facilitating aberrant FGF2-mediated signaling and cellular outgrowth, we next sought to establish a pharmacologic means to inhibit this process. Addition of three different FGFR inhibitors for 18 hours before stimulation with FGF2 demonstrated the enhanced durability of our recently described covalent inhibitor of FGFR (FIIN-2) to block the function of this receptor as compared with a reversible FGFR inhibitor (BGJ-398) in metastatic D2.A1 cells (Fig. 5A and Supplementary Fig. S3C). However, FIIN-2 only showed moderate mouse liver microsomal (MLM) stability ($T_{1/2}$= 4.0 minutes), precluding its further development as a drug candidate. Further optimization of FIIN-2 lead to the formulation of FIIN-4, which showed rather improved MLM stability ($T_{1/2}$= 16.6 minutes), and maintained good enzymatic and cellular IC_{50}s against FGFR1–4 as well as a similar kinase selectivity profile as FIIN-2 (Supplementary Fig. S4A and S4B; Supplementary Table S3). FIIN-4 also demonstrated good overall pharmacokinetic properties, with $T_{1/2}$of 2.4 hours, an AUC value of 935 ng/hr/mL following a 10 mg/kg oral dose and moderate oral bioavailability of 31% (Supplementary Fig. S4C). Similar to FIIN-2, FIIN-4 also demonstrated robust long-term inhibition of FGFR signaling in the D2.A1 cells (Fig. 5A). Treatment with FIIN-4 did not affect the ability of EGF to induce Erk1/2 phosphorylation or increase the 3D growth of NMuMG cells, demonstrating the specificity of this compound for FGFR (Supplementary Fig. S5). In addition to directly targeting FGFR, we also investigated the potential downstream mechanisms of FGFR:β3 integrin signaling by using two different inhibitors of FAK, PF-562,271/VS-6062 (PF-271) and VS-6063 (defactinib). Long-term inhibition of FAK using both compounds inhibited FGF2-mediated phosphorylation of Erk1/2 in a dose-dependent fashion (Fig. 5B and C). Moreover, a short-term pretreatment (10 minutes) with defactinib was also highly effective at blocking FGF2-mediated phosphorylation of Erk1/2 (Fig. 5D). The importance of robust long-term inhibition of FGFR signaling is emphasized by the fact that covalent inhibition of FGFR led to decreased 3D outgrowth following a single dose of inhibitor, results that were not observed with the competitive inhibitor, BGJ-398 (Fig. 5E). Defactinib was similarly capable of blocking overall 3D outgrowth after only a single dose of this compound (Fig. 5E and F). Finally, treatment

Published OnlineFirst July 1, 2016; DOI: 10.1158/1535-7163.MCT-16-0136

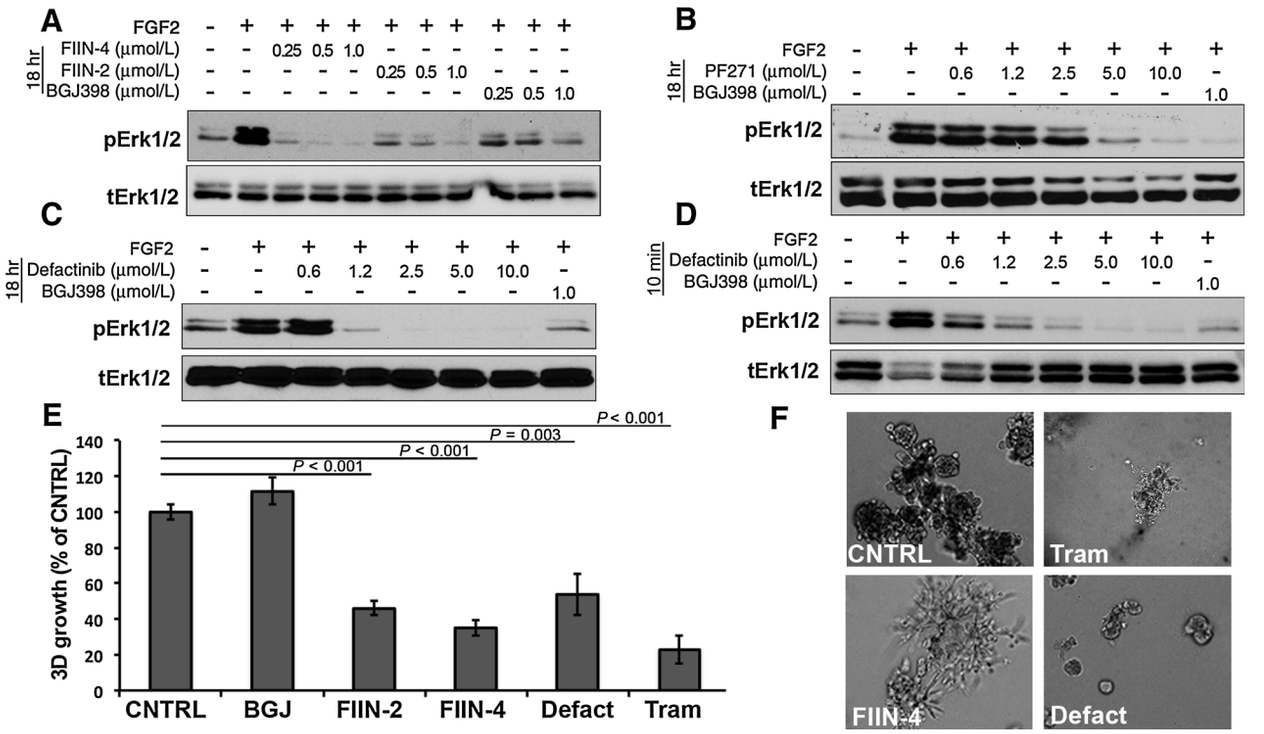

Figure 5.

Pharmacologic inhibition of FAK blocks FGF2:Erk1/2 signaling. **A,** D2.A1 cells were pretreated for 18 hours with the covalent FGFR inhibitors FIIN-4 or FIIN-2, or the Type I FGFR inhibitor BGJ-398 at the indicated concentrations. **B** and **C,** D2.A1 cells were pretreated for 18 hours with the indicated concentration of the FAK inhibitors PF-271 or Defactinib. **D,** D2.A1 cells were pretreated for 10 minutes with indicated concentrations of Defactinib. In **A–D,** cells were serum starved for 18 hours with or without inhibitor pretreatment and cells were subsequently stimulated with FGF2 (20 ng/mL) for 30 minutes and analyzed by immunoblot for downstream phosphorylation of Erk1/2. Expression of total Erk1/2 was analyzed as a loading control. **E,** D2.A1 cells were grown in 3D culture for 4 days at which point a single treatment with the indicated inhibitors of FGFR (BGJ, FIIN-2, FIIN-4), FAK (Defact), or MEK1/2 (Tram) were added for 4 days. Following this treatment period cells were allowed to grow for an additional 4 days and luminescence was quantified. Changes in cellular outgrowth are shown as a percentage relative to the untreated control (CNTRL) luminescence value. Data are the mean values ±SE of at least six replicates completed over at least two independent experiments resulting in the indicated *P* values. **F,** brightfield photomicrographs of final 3D cell clusters formed after the total 12 days of growth. These images were collected using a TS100 Nikon microscope at ×100 magnification.

with trametinib, an FDA-approved allosteric inhibitor of MEK1/2, was similarly capable of inhibiting the 3D outgrowth of the D2.A1 cells and completely blocked the ability of FGF2 to induce outgrowth of our FGFR1 overexpressing NMuMG cells (Fig. 5E and Supplementary Fig. S5). Taken together with our previous findings, these data strongly suggest that FAK is functioning downstream of β3 integrin and FGFR1 to facilitate an FGF2:Erk1/2 signaling axis and outgrowth of metastatic breast cancer cells.

Covalent targeting of FGFR blocks metastatic tumor growth

We next sought to specifically evaluate the role of FGFR:β3 signaling in the metastatic tumor microenvironment. We have recently demonstrated that the 4T1 model of advanced stage breast cancer undergoes a spontaneous EMT during *in vivo* metastasis as compared with the epithelial phenotype of these cells when cultured *in vitro*(12, 23). Consistent with these findings, *ex vivo* RT-PCR analyses clearly demonstrate that a clonal, luciferase-expressing 4T1 cell line (4T1-L4) displayed robust upregulation of FGFR1 following pulmonary metastasis from the mammary fat pad (Fig. 6A and Supplementary Fig. S6). Further expression analyses between *in vitro* and *ex vivo* 4T1-L4 lung metastases demonstrated enhanced expression of β3 integrin, and indicated the upregulation of all the major isoforms of FGFR1 (Fig. 6A). Along these lines, FIIN-2 and FIIN-4 potently inhibited cellular viability of *ex vivo* 4T1-L4 pulmonary metastases (Fig. 6B). In contrast, similar experiments showed no effect of FIIN molecules on cell viability of normal murine mammary gland cells (data not shown). Consistent with these viability data, FIIN-2 and FIIN-4 abrogated the constitutive phosphorylation of Erk1/2 in *ex vivo* 4T1-L4 pulmonary metastases, even at low nanomolar concentrations (Fig. 6C). We also specifically monitored organotypic, 3D tumor cell growth within these heterogeneous *ex vivo* cultures via their stable expression of firefly luciferase, in which treatment with FIIN-2 or FIIN-4 led to a dramatic eradication of tumor cells (Fig. 6D and E). To evaluate the *in vivo* efficacy of FIIN-4, *ex vivo* 4T1-L4 pulmonary metastases were reinoculated into the pulmonary microenvironment of fresh cohorts of mice via a tail vein injection, and pulmonary tumor growth was quantified by bioluminescence (Fig. 6F). Forty-eight hours after metastatic inoculation, we initiated FIIN-4 therapy via oral gavage. Consistent with our 3D culture data, *in vivo* FIIN-4 therapy led to a potent inhibition of pulmonary tumor growth (Fig. 6F and G). Fifteen days after tail vein inoculation, the first control mouse was sacrificed due to pulmonary tumor burden, at which point FIIN-4 treatments were

Published OnlineFirst July 1, 2016; DOI: 10.1158/1535-7163.MCT-16-0136

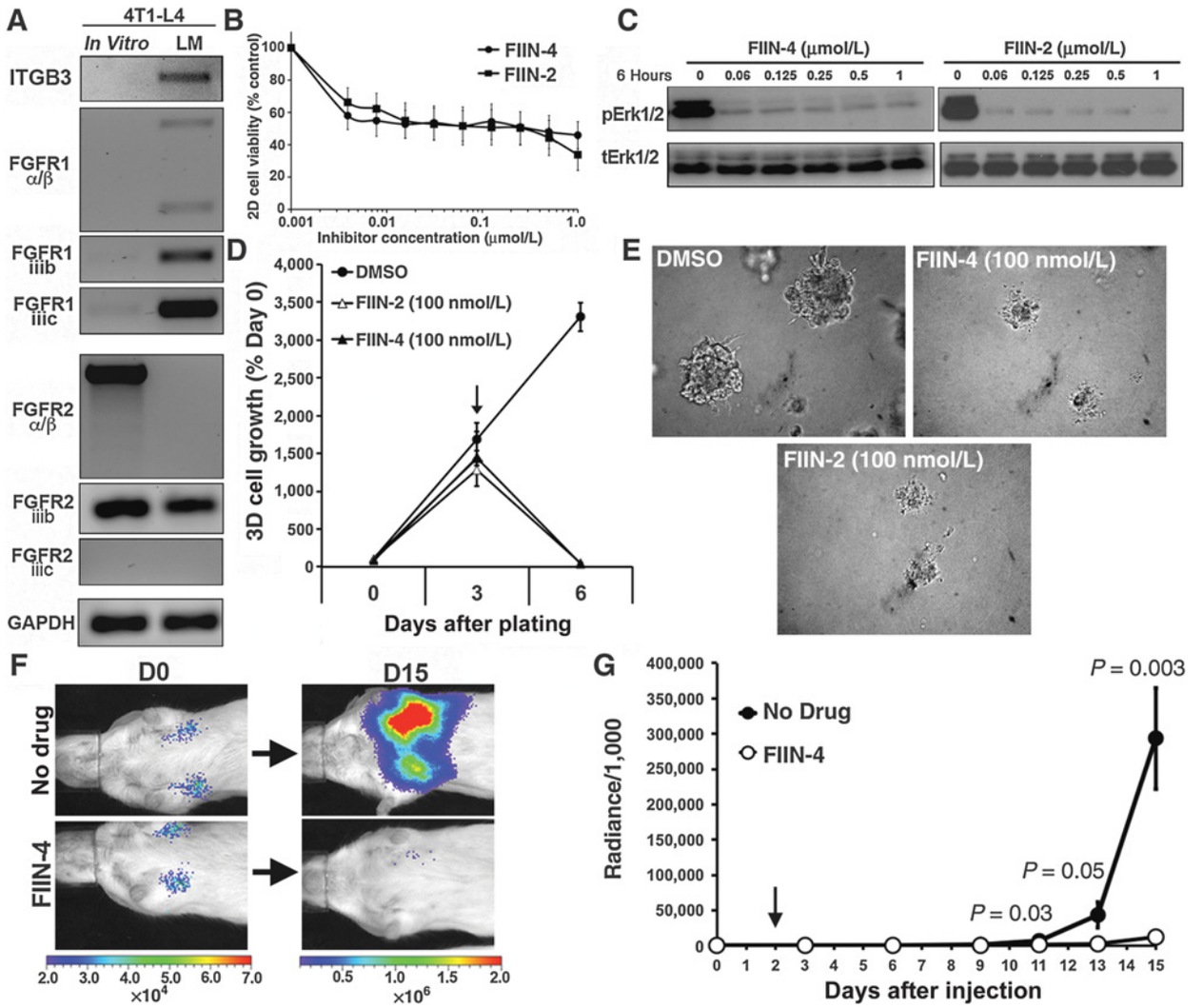

Figure 6.

FIIN-4 potently inhibits pulmonary metastases. **A,** clonal 4T1-L4 cells were used to form orthotopic mammary tumors and the resultant lung metastases (LM) were analyzed *ex vivo* by RT-PCR for expression of β3 integrin (ITGB3) and various isoforms of FGFR1 and FGFR2 as compared with their *in vitro* parental counterparts. Analysis of GAPDH served as a loading control. **B,** *ex vivo* 4T1-L4 lung metastases were cultured on plastic in the presence of the indicated concentrations for the covalent FGFR inhibitors FIIN-2 or FIIN-4 for 48 hours. Data are the mean ± SE of three independent experiments normalized to no inhibitor, control values. **C,** *ex vivo* 4T1-L4 lung metastases were treated with the indicated concentrations of FGFR inhibitors for 6 hours. These cultures were subsequently analyzed by immunoblot for downstream phosphorylation of Erk1/2. Expression of total Erk1/2 served as a loading control. **D,** *Ex vivo* 4T1-L4 lung metastases were grown under 3D culture conditions for 3 days at which point FIIN-2 or FIIN-4 were added to the cultures (arrow). Tumor cell–specific 3D outgrowth was quantified by firefly luminescence. Data are normalized to the plated values and are the mean of three independent experiments completed in triplicate. **E,** photomicrographs showing inhibition of 3D growth of the *ex vivo* 4T1-L4 metastases under control conditions (DMSO) and in the presence of the indicated concentrations of FGFR inhibitors. These brightfield images were collected using a TS100 Nikon microscope at ×40 magnification. **F,** *ex vivo* 4T1-L4 lung metastases were re-inoculated into the tail vein of female Balb/C mice. 48 hours after injection cohorts of mice were left untreated (No drug) or were treated with FIIN-4 (25mg/kg/48 h) via oral gavage. Shown are bioluminescent images of representative mice from each group immediately following tail vein inoculation (D0) and 15 days after inoculation (D15).**G,** data are the mean ± SE of the bioluminescence (Radiance) values of 5 mice per treatment group as described in **F,** resulting in the indicated *P* values between the untreated and FIIN-4 therapy groups.

stopped. Even with this discontinuation of therapy, FIIN-4 still resulted in a highly significant prolongation in survival (Supplementary Fig. S7). Taken together, these findings clearly demonstrate that FGFR is a major driver of EMT-associated metastatic outgrowth and its function can be successfully antagonized within the metastatic microenvironment through the systemic administration of FIIN-4.

FIIN-4 effectively targets chemotherapy resistant, metastatic TNBC

To verify the clinical significance of an FGFR:β3 integrin complex in breast cancer progression, we analyzed patient survival rates upon cohort bifurcation based on the mean expression value of FGFR, FAK (*PTK2*), and β3 integrin (*ITGB3*). Analysis of a cohort of basal-like breast cancer patients revealed that β3 integrin

Published OnlineFirst July 1, 2016; DOI: 10.1158/1535-7163.MCT-16-0136

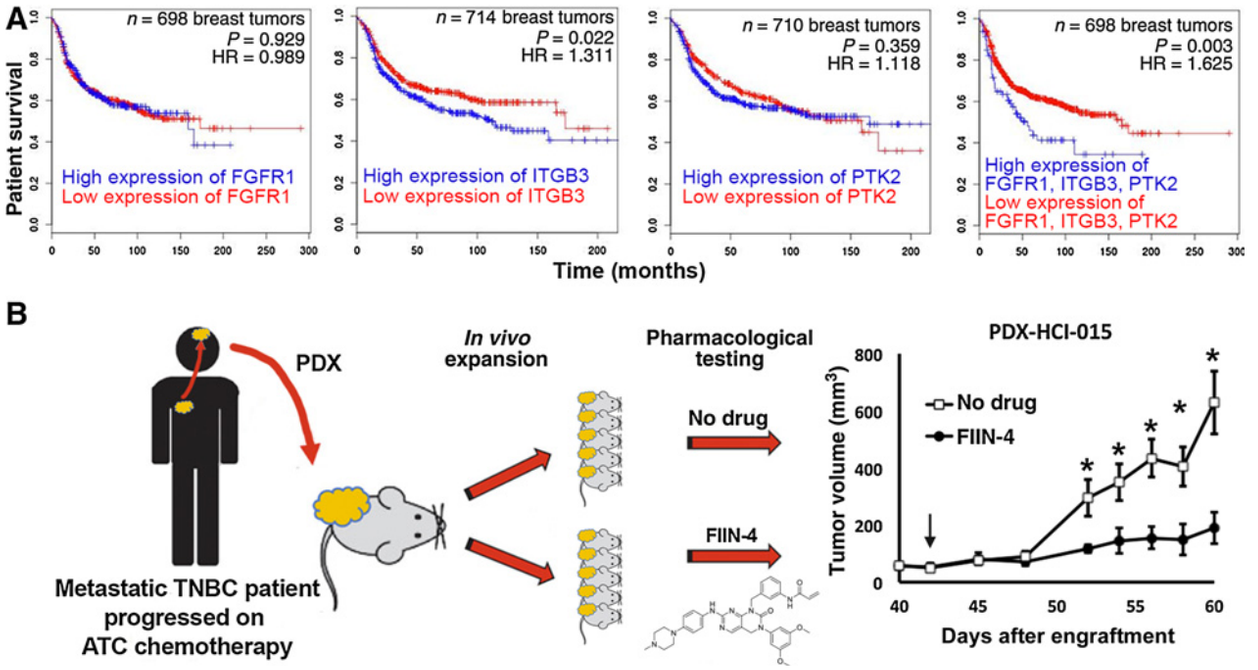

Figure 7.

FIIN-4 effectively targets chemoresistant metastatic TNBC. **A,** patient cohorts bearing basal-like breast tumors were separated into two groups based on the mean expression value of the indicated single genes [*FGFR1*, *ITGB3*, or *PTK2* (FAK)] or as a signature of all three genes together and patient survival was analyzed. The number of patients for each analysis is indicated, resulting in the indicated *P* values and hazard ratios (HR). **B,** a patient-derived xenograft was established from triple-negative brain metastases that progressed on ATC chemotherapy. These tumors were expanded via surgical procedures and tumor-bearing mice were split into two cohorts of 5 mice each, one of which was treated with FIIN-4 (25 mg/kg/48hr) via oral gavage (initiation of treatment is indicated by the black arrow). Tumor volumes were measured at the indicated time points. Data are presented as the mean tumor volume ± the SE, where *, $P \leq 0.01$ between the control and FIIN-4 treatment groups.

expression alone was associated with a significant decrease in patient survival rates, but FAK and FGFR1 alone were not (Fig. 7A). However, combination of these three genes into a signature led to a more robust separation between high and low expressing tumors (Fig. 7A; right). FGFR3 or FGFR4 also led to more robust bifurcation in patient survival when combined with β3 integrin and FAK (Supplementary Fig. S8). Consistent with the depletion of FGFR2 through EMT and metastasis, addition of FGFR2 to this signature nullified the ability of β3 integrin to predict for patient survival (Supplementary Fig. S8). To further support these data, TNBC brain metastases were harvested from a patient whose disease had progressed while receiving adramycin, taxol, cyclophosphamide (ATC) chemotherapy. These PDX tissues were expanded to 10 individual mice and randomized into two groups 40 days after engraftment. Those mice that received FIIN-4 demonstrated a significant delay in tumor growth as compared to the control group (Fig. 7B). Taken together, with our mechanistic data these findings strongly suggest that EMT-mediated expression of FGFR1 and β3 integrin work in complex through the activity of FAK to drive metastatic tumor growth.

Discussion

In this study, we have developed a first-in-class covalent inhibitor of FGFR that is capable of blocking the *in vivo* growth of TNBC within anatomically relevant metastatic locations. Mechanistically, we demonstrate that EMT drives the expression of β3 integrin and FGFR1, both of which are necessary for enhanced response to FGF2 (Fig. 8; refs. 1, 28). FIIN-4 demonstrated excellent efficacy against the cell lines and tumor tissues studied herein, and our current dosing schedule (25 mg/kg/48 h via oral gavage) did not result in any overt toxicity to the animals. However, a major hurdle to the clinical application of FIIN-4 will be diagnostic selection of the proper TNBC patient populations. Our patient and mechanistic data begin to shed light on this problem by suggesting that expression levels of β3 integrin, FAK and FGFR1, 3, and 4 could serve as potential biomarkers for prescription of FIIN-4. Ongoing work in the laboratory is applying FIIN-4 to a growing set of PDX samples. Overtime we will be able to correlate several pieces of annotated data, including breast cancer subtype, previous therapy, global gene expression and protein localization data with tumor response to FIIN-4. Of particular importance may be the subcellular localization of FGFR1. Our data herein, previous studies from our laboratory and others, and samples contained in the Human Protein Atlas clearly demonstrate that in addition to plasma membrane signaling FGFR1 can localize to the nucleus where it can influence the expression of hundreds of genes (1, 30, 31). Therefore, nuclear localization of FGFR1 may serve as an important biomarker for efficacy/resistance to FIIN-4. In any event, it is encouraging that our current studies clearly demonstrate that FIIN-4 is capable of inhibiting the growth of metastatic TNBC that had progressed on chemotherapy.

The connection of integrins and the extracellular matrix to downstream signaling events often involves both the scaffolding

Published OnlineFirst July 1, 2016; DOI: 10.1158/1535-7163.MCT-16-0136

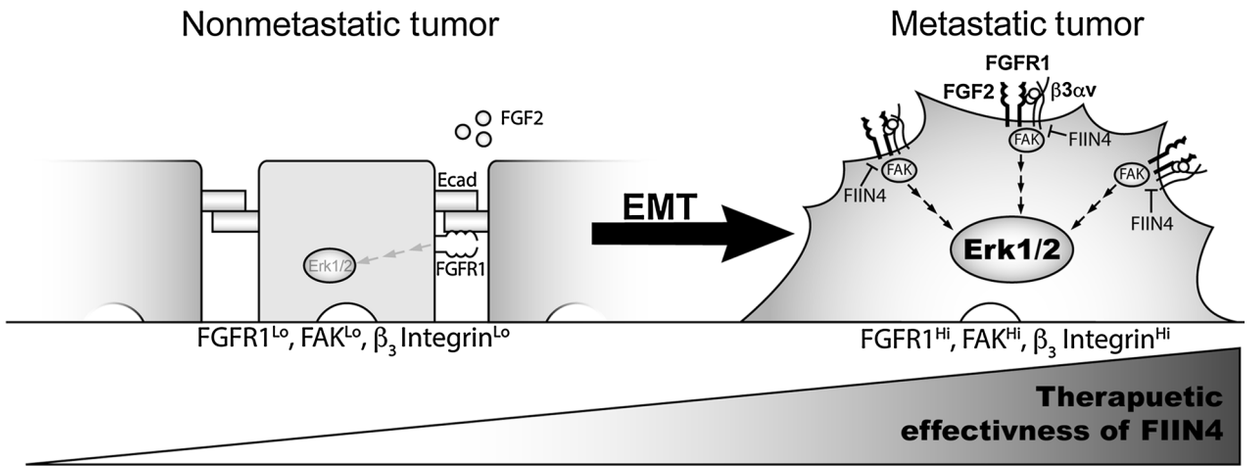

Figure 8.

A schematic representation of how the processes of EMT drive FGFR-dependent growth of breast cancer metastases. In epithelial-like tumor cells FGFR1-iiic levels are low and interactions with E-cadherin limit the ability of FGF2 to stimulate Erk1/2, preventing cell growth. However, following EMT, expression levels of FGFR1-iiic and β3 integrin are increased, producing multiple signaling complexes that use FAK to aberrantly activate Erk1/2. These molecular events promote metastatic tumor growth, but they also can be used to effectively identify those patients that will respond to FIIN4 therapy, our newly developed covalent inhibitor of FGFR.

and kinase function of FAK. In this study, we demonstrate the ability of two distinct FAK inhibitors, Defactinib and PF-271, to inhibit *in vitro* FGF2 signaling. These data suggest that coadministration of FGFR and FAK inhibitors could provide an improved therapeutic response. However, the clinical utility of FAK inhibitors has been limited by their pharmacokinetics and solubility (32). Along these lines, the COMMAND trial (NCT01870609) evaluating defactinib for the treatment of malignant pleural mesothelioma was recently terminated due to lack of efficacy. Furthermore, systemic inhibition of FAK can inhibit T-cell function, and immune cell infiltration which may detract from its tumor cell–autonomous effects (20, 33). Because of these reasons this study did not pursue combination therapies targeting both FAK and FGFR.

Recent findings point to engagement of the extracellular matrix and activation of Erk1/2 signaling as key mechanisms that are required for disseminated breast cancer cells to overcome systemic dormancy and undergo metastatic outgrowth (34, 35). Our data support and expand upon these findings by demonstrating that FGFR in complex with β3 integrin acts as a key upstream mediator of Erk1/2 activation. Indeed, our data in Fig. 3 demonstrate that β3 integrin levels dramatically increase in all 3D culture conditions compared with tissue culture plastic, and this increase was somewhat inhibited by the addition of collagen I. These findings are consistent with the notion that FGFR1:β3 integrin signaling complexes are enhanced in more compliant metastatic microenvironments such as the lungs or liver. Whether the mechanisms of β3 integrin regulation by matrix compliance are related to or independent from the ability of EMT to mediate β3 integrin expression remains to be definitively determined (23).

Overall our studies herein add important mechanistic understanding to how the processes of EMT drive integrins and growth factor receptors to work in concert during the metastatic progression of breast cancer. Going beyond these mechanistic data, we used both patient-derived xenografts and a highly aggressive syngeneic model of metastatic breast cancer growing within the pulmonary microenvironment to demonstrate the robust *in vivo* utility of FIIN-4, a first-in-class covalent inhibitor of FGFR. Finally, we identify a β3 integrin:FAK:FGFR molecular signature that is capable of indicating a poor prognosis group of basal-like breast cancer patients that would clearly benefit from FIIN-4 therapy. These findings strongly support the clinical advancement of this exciting therapeutic strategy.

Disclosure of Potential Conflicts of Interest

No potential conflicts of interest were disclosed.

Authors' Contributions

Conception and design: W. Brown, N.S. Gray, M.K. Wendt
Development of methodology: W. Brown, M.K. Wendt
Acquisition of data (provided animals, acquired and managed patients, provided facilities, etc.): W. Brown, L. Tan, A. Smith, N.S. Gray, M.K. Wendt
Analysis and interpretation of data (e.g., statistical analysis, biostatistics, computational analysis): W. Brown, L. Tan, A. Smith, M.K. Wendt
Writing, review, and/or revision of the manuscript: W. Brown, L. Tan, N.S. Gray, M.K. Wendt
Administrative, technical, or material support (i.e., reporting or organizing data, constructing databases): W. Brown, M.K. Wendt
Study supervision: M.K. Wendt

Acknowledgments

The authors thank the members of the Wendt Laboratory for critical reading of the article. The authors also thank Dr. David Lum for his assistance in acquiring patient-derived tumor tissues and the authors acknowledge the expertise of the personnel within the Purdue Center for Cancer Research Biological Evaluation Core (P30 CA023168).

Grant Support

This research was supported in part by the NIH (R00 CA166140) and the Showalter Trust Foundation (to M.K. Wendt) and by Lung SPORE grant (P50 CA090578; to N.S. Gray).

The costs of publication of this article were defrayed in part by the payment of page charges. This article must therefore be hereby marked *advertisement* in accordance with 18 U.S.C. Section 1734 solely to indicate this fact.

Received March 9, 2016; revised May 11, 2016; accepted May 31, 2016; published OnlineFirst July 1, 2016.

Published OnlineFirst July 1, 2016; DOI: 10.1158/1535-7163.MCT-16-0136

References

1. Wendt MK, Taylor MA, Schiemann BJ, Sossey-Alaoui K, Schiemann WP. Fibroblast growth factor receptor splice variants are stable markers of oncogenic transforming growth factor β1 signaling in metastatic breast cancers. Breast Cancer Res 2014;16:R24.
2. Azuma K, Tsurutani J, Sakai K, Kaneda H, Fujisaka Y, Takeda M, et al. Switching addictions between HER2 and FGFR2 in HER2-positive breast tumor cells: FGFR2 as a potential target for salvage after lapatinib failure. Biochem Biophys Res Commun 2011;407:219–24.
3. Dey JH, Bianchi F, Voshol J, Bonenfant D, Oakeley EJ, Hynes NE. Targeting fibroblast growth factor receptors blocks PI3K/AKT signaling, induces apoptosis, and impairs mammary tumor outgrowth and metastasis. Cancer Res 2010;70:4151–62.
4. Sharpe R, Pearson K A, Herrera-Abreu MT, Johnson D, Mackay A, Welti JC, et al. FGFR signaling promotes the growth of triple negative and basal-like breast cancer cell lines both *in vitro* and *in vivo*. Clin Cancer Res 2011;17:5275–86.
5. Holzmann K, Grunt T, Heinzle C, Sampl S, Steinhoff H, Reichmann N, et al. Alternative splicing of fibroblast growth factor receptor IgIIIloops in cancer. J Nucleic Acids 2012;2012:950508.
6. ElbauomyElsheikh S, Green AR, Lambros MBK, Turner NC, Grainge MJ, Powe D, et al. FGFR1 amplification in breast carcinomas: a chromogenic *in situ* hybridisation analysis. Breast Cancer Res 2007;9:R23.
7. Shapiro IM, Cheng AW, Flytzanis NC, Balsamo M, Condeelis JS, Oktay MH, et al. An EMT-driven alternative splicing program occurs in human breast cancer and modulates cellular phenotype. PLoS Genet 2011;7:e1002218.
8. Warzecha CC, Jiang P, Amirikian K, Dittmar KA, Lu H, Shen S, et al. An ESRP-regulated splicing programme is abrogated during the epithelial-mesenchymal transition. EMBO J 2010;29:3286–300.
9. Brooks MD, Burness ML, Wicha MS. Therapeutic implications of cellular heterogeneity and plasticity in breast cancer. Cell Stem Cell 2015;17:260–71.
10. Tam WL, Weinberg RA. The epigenetics of epithelial-mesenchymal plasticity in cancer. Nat Med 2013;19:1438–49.
11. Wendt MK, Tian M, Schiemann WP. Deconstructing the mechanisms and consequences of TGF-β-induced EMT during cancer progression. Cell Tissue Res 2012;347:85–101.
12. Wendt MK, Smith JA, Schiemann WP. Transforming growth factor-β-induced epithelial-mesenchymal transition facilitates epidermal growth factor-dependent breast cancer progression. Oncogene 2010;29:6485–98.
13. Galliher AJ, Schiemann WP. Beta3 integrin and Src facilitate transforming growth factor-beta mediated induction of epithelial-mesenchymal transition in mammary epithelial cells. Breast Cancer Res 2006;8:R42.
14. Mori S, Wu C-Y, Yamaji S, Saegusa J, Shi B, Ma Z, et al. Direct binding of integrin alphavbeta3 to FGF1 plays a role in FGF1 signaling. J Biol Chem 2008;283:18066–75.
15. Rusnati M, Tanghetti E, Dell'Era P, Gualandris A, Presta M. $\alpha v\beta 3$ integrin mediates the cell-adhesive capacity and biological activity of basic fibroblast growth factor (FGF-2) in cultured endothelial cells. Mol Biol Cell 1997;8:2449–61.
16. Mori S, Takada Y. Crosstalk between fibroblast growth factor (FGF) receptor and integrin through direct integrin binding to FGF and resulting integrin-FGF-FGFR ternary complex formation. Med Sci 2013;1:20–36.
17. Liu Q, Sabnis Y, Zhao Z, Zhang T, Buhrlage SJ, Jones LH, et al. Developing irreversible inhibitors of the protein kinase cysteinome. Chem Biol 2013;20:146–59.
18. Hirsh V. Next-generation covalent irreversible kinase inhibitors in NSCLC: focus on afatinib. Biodrugs 2015;29:167–83.
19. Tan L, Wang J, Tanizaki J, Huang Z, Aref AR, Rusan M, et al. Development of covalent inhibitors that can overcome resistance to first-generation FGFR kinase inhibitors. Proc Natl Acad Sci U S A 2014;111:E4869–4877.
20. Wendt MK, Schiemann WP. Therapeutic targeting of the focal adhesion complex prevents oncogenic TGF-beta signaling and metastasis. Breast Cancer Res 2009;11:R68.
21. Parvani JG, Galliher-Beckley AJ, Schiemann BJ, Schiemann WP. Targeted inactivation of β1 integrin induces β3 integrin switching, which drives breast cancer metastasis by TGF-β. Mol Biol Cell 2013;24:3449–59.
22. DeRose YS, Gligorich KM, Wang G, Georgelas A, Bowman P, Courdy SJ, et al. Patient-derived models of human breast cancer: protocols for *in vitro* and *in vivo* applications in tumor biology and translational medicine. Curr Protoc Pharmacol 2013;14:Unit 14.23.
23. Wendt MK, Taylor MA, Schiemann BJ, Schiemann WP. Down-regulation of epithelial cadherin is required to initiate metastatic outgrowth of breast cancer. Mol Biol Cell 2011;22:2423–35.
24. Berglund L, Björling E, Oksvold P, Fagerberg L, Asplund A,Szigyarto CA-K, et al. A genecentric Human Protein Atlas for expression profiles based on antibodies. Mol Cell Proteomics 2008;7:2019–27.
25. Uhlen M, Oksvold P, Fagerberg L, Lundberg E, Jonasson K, Forsberg M, et al. Towards a knowledge-based Human Protein Atlas. Nat Biotechnol 2010;28:1248–50.
26. Li X, He Y, Ruiz CH, Koenig M, Cameron MD, Vojkovsky T. Characterization of dasatinib and its structural analogs as CYP3A4 mechanism-based inactivators and the proposed bioactivation pathways. Drug Metab Dispos 2009;37:1242–50.
27. Wendt MK, Schiemann BJ, Parvani JG, Lee Y-H, Kang Y, Schiemann WP. TGF-β stimulates Pyk2 expression as part of an epithelial-mesenchymal transition program required for metastatic outgrowth of breast cancer. Oncogene 2013;32:2005–15.
28. Shirakihara T, Horiguchi K, Miyazawa K, Ehata S, Shibata T, Morita I, et al. TGF-β regulates isoform switching of FGF receptors and epithelial–mesenchymal transition. EMBO J 2011;30:783–95.
29. Shibue T, Weinberg RA. Integrin beta1-focal adhesion kinase signaling directs the proliferation of metastatic cancer cells disseminated in the lungs. Proc Natl Acad Sci U S A 2009;106:10290–5.
30. Stachowiak MK, Stachowiak EK. Evidence-based theory for integrated genome regulation of ontogeny—an unprecedented role of nuclear FGFR1 signaling. J Cell Physiol 2016;231:1199–218.
31. Terranova C, Narla ST, Lee Y-W, Bard J, Parikh A, Stachowiak EK, et al. Global developmental gene programing involves a nuclear form of fibroblast growth factor receptor-1 (FGFR1). PLoS ONE 2015;10: e0123380.
32. Infante JR, Camidge DR, Mileshkin LR, Chen EX, Hicks RJ, Rischin D, et al. Safety, pharmacokinetic, and pharmacodynamic phase I dose-escalation trial of PF-00562271, an inhibitor of focal adhesion kinase, in advanced solid tumors. J Clin Oncol 2012;30:1527–33.
33. Wiemer AJ, Wernimont SA, Cung T-D, Bennin DA, Beggs HE, Huttenlocher A. The focal adhesion kinase inhibitor PF-562,271 impairs primary CD4+ T cell activation. Biochem Pharmacol 2013;86:770–81.
34. El Touny LH, Vieira A, Mendoza A, Khanna C, Hoenerhoff MJ, Green JE. Combined SFK/MEK inhibition prevents metastatic outgrowth of dormant tumor cells. J Clin Invest 2014;124:156–68.
35. Barkan D, Green JE, Chambers AF. Extracellular matrix: a gatekeeper in the transition from dormancy to metastatic growth. Eur J Cancer 2010;46: 1181–8.

Published OnlineFirst July 1, 2016; DOI: 10.1158/1535-7163.MCT-16-0136

AACR American Association for Cancer Research

Molecular Cancer Therapeutics

Covalent Targeting of Fibroblast Growth Factor Receptor Inhibits Metastatic Breast Cancer

Wells S. Brown, Li Tan, Andrew Smith, et al.

Mol Cancer Ther 2016;15:2096-2106. Published OnlineFirst July 1, 2016.